Turbulence Mixed Convective Nanofluid Flow over Double Forward-Facing Steps: A Numerical Simulation Study

Open Access

Omar Assi Hussein[1,2], Khairul Habib[1], Ali Samer Muhsan[3,*]

1   Department of Mechanical Engineering, College of Engineering, Universiti Teknologi PETRONAS, 32610 Seri Iskandar, Perak Darul Ridzuan, Malaysia
2   Department of Mechanical Engineering, College of Engineering, Tikrit Universiti, IRAQ
3   Department of Petroleum Engineering, College of Engineering, Universiti Teknologi PETRONAS, 32610 Seri Iskandar, Perak Darul Ridzuan, Malaysia

ARTICLE INFO	ABSTRACT
	Predictions are reported for mixed convection using various types of nanofluids over forward-facing double steps in a duct. The continuity, momentum and energy equations are discretized and the simple algorithm is applied to link the pressure and flow fields inside the domain. Different types of nanoparticles Al_2O_3, CuO, SiO_2 and ZnO, with different volume fractions in range of 1-4% and different nanoparticles diameter in the range of $20 - 80$ nm in base fluid (water, glycerin, engine oil and ethylene glycol) were used. Numerical investigations are conducted using finite volume method. In this study, different parameters such as the geometrical specifications (different steps heights in the range of $h_1 = 0.01m$-$0.04m$ and $h_2 = 0.03m$-$0.06m$ for FFS) are used. Different Reynolds numbers in the range of 4000-100000 (turbulent flow) are investigated to identify their effects on the heat transfer and fluid characteristics. The results indicate that SiO_2-water has the highest Nusselt number followed by Al_2O_3-water, CuO-water and ZnO-water. The Nusselt number increases as the volume fraction increases but it decreases as the nanoparticles diameter increases. The velocity magnitude increases as the density of nanofluids decreases. The recirculation region and the Nusselt number increase as the step height, Reynolds number, and the volume fraction increase.

1. Introduction

Mixed convection heat transfer in forward facing double steps had been a subject of interest in many research studies. By adding increase of discretion points to the simulation, and the power of the computers devices have been improving in terms of memory and speed capability. Therefore, the implementation of numerical simulation is best than both experimental and theoretical approaches. It eschews the annoying measurements in full-scale experimental devices, and the

---

*   Corresponding author.
E-mail address: alisameer2007@gmail.com (Ali Samer Muhsan)

equipment cost, and time spent for the setups constructions. So, numerical simulation were defined as the third approach which containing the two (experimental and theoretical) approaches for studying the physical laws [1]. One of the ways to enhance heat transfer in the separated regions is to employ nanofluids. Nanofluids are fluids that contain suspended nanoparticles such as metals and oxides. These nanoscale particles keep suspended in the base fluid. Thus, it does not cause an increase in pressure drop in the flow field. Past studies showed that nanofluids exhibit enhanced thermal properties, such as higher thermal conductivity and convective heat transfer coefficients compared to the base fluid; see, for example, Daungthongsuk and Wongwises [2], Wang Mujumdar [3], Mohammed *et al.,* [4], Fathinia and Ahmed Kadhim Hussein [5]. Abu-Mulaweh *et al.,* [6-7], and Omar *et al.,* [8], conducted measurements are for laminar mixed convection flow buoyancy-opposing two-dimensional flow over a vertical forward-facing step. The upstream wall of the step was an adiabatic surface, while both the downstream wall and the step were heated to a uniform temperature that was higher than temperature of the approaching air. The measurements were carried out for a step height of 0.8 cm. It was observed that the laminar non-circulating flow region downstream of the step, the local Nusselt number decreased inside the recirculating flow region as the opposing buoyancy force increased.

Chiba *et al.,* [9], Saqar *et al.,*[10] conducted flow observations over a forward-facing step channel to predict the mechanism for instability of planar entry flow of the types of unstable flow patterns. Furthermore, the coalescence and appearance of the Goertler vortex pairs cause their fourth-and-back movement along the longitudinal direction of the channel, and three-dimensional lip vortices play an important role in the appearance of a pair of the Goertler vortices.

Hirofumi and Yasutaka [11] investigated turbulent flow system of a boundary layer over a forward-facing step. It was shown that pronounced counter-gradient diffusion phenomena (CDP) were especially noted on the step near from the wall. Thus, the Reynolds numbers based on the step height became Re_h= 900 - 3000. Therefore, the detailed structure of the results of DNS can be applied to the improvement of the turbulence model and turbulent boundary layer over a forward-facing step.

Largeau and Moriniere [12] carried out measurements of aerodynamic fields and wall pressure fluctuations in separated flows over a forward facing. It was resulted that a different behavior of the flow depending on the aspect ratio l/h and δ/h for high Reynolds numbers. The Reynolds number Re_h varies from 2.88×10^4 (h = 30 mm, U_e = 15 m/s) to 12.82×10^4 (h = 50 mm, U_e = 40 m/s). It was noted that the flapping motion (low frequency) at the separation play an important role and the large scale structures in the shear layer in the generation of the wall pressure fluctuations rather than the near wall pattern bounded in the recirculation zone.

Yilmaz and Oztop [13] presented heat transfer of turbulent forced convection for double forward facing step flow. The standard $k-\varepsilon$ turbulence model was employed to get turbulence flow modeling. Effects of fluid flow step, Reynolds numbers and step lengths on heat transfer and heights were investigated. It was revealed that the heat transfer and turbulent intensity are increased with higher Re.

Very few number of research works were conducted numerically and experimentally by Dutta and Dutta [14], Yang and Huang [15], and Omar A. Hussein [16], to capture more detail of the fluid flow pattern and heat transfer phenomena in the channel with perforated baffle. Three-dimensional laminar convection flow adjacent to backward-facing step in a heated rectangular duct with a baffle mounted on the upper wall was numerically simulated by Nie *et al.,* [17].

The problem of laminar flow over backward-facing step geometry in natural, forced, and mixed convection has been investigated extensively in the past, both numerically and experimentally by Lin

et al., [18], Hong *et al.,* [19], and Mohammed [20], and the references cited therein. On the other hand, the problem of laminar flow over a forward-facing step has received very little attention.

Chiang *et al.,* [21] investigated developed three-dimensional channel flow expanded into the channel with an expansion ratio of 1.94. Numerical solutions for this backward-facing step problem were gotten on the basis of Reynolds numbers as high as 800, the step height, 0.942. It was observed that the rigorous mathematical foundation had facilitated the determination of the separation, continuously and separation line on the floor with the attachment line, on the roof of the channel.

The first numerical study to investigate the flow and heat transfer over a backward-facing step using nanofluids was done by Abu-Nada [22]. The Reynolds number and nanoparticles volume fraction used were in the range of $200 \leq Re \leq 600$ and $0 \leq \emptyset \leq 0.2$, respectively, for five types of nanoparticles which are Cu, Ag, Al_2O_3, CuO, and TiO_2. He reported that the high Nusselt number inside the recirculation zone mainly depended on the thermophysical properties of the nanoparticles and it is independent of Reynolds number.

The study of steady laminar mixed convection flow over double forward-facing steps utilizing nanofluids in a two-dimensional horizontal configuration under uniform heat flux boundary conditions seems not to have been investigated in the past and this has motivated the present study. Thus, the present study deals with different types of nanofluids such as (Al_2O_3, CuO, SiO2, and ZnO) with different volume fractions and different nanoparticle diameters. The effects of heat flux and Reynolds number on the velocity distribution, skin friction coefficient, and Nusselt number are studied and reported to illustrate the effect nanofluids on these parameters for flows.

2. Numerical Model
2.1 Physical Model

Considering the forward double facing steps placed in channel as shown in Figure 1 as a representation of a mixed convective flow. The wall downstream of the step (a) is maintained at a uniform wall heat flux (q_x), while the straight wall that forms the other side of the channel is maintained at constant temperature equivalent to the inlet fluid temperature (T_{in}). The wall downstream of the step (b, c) and the step it-self (h_1,h_2) are considered as adiabatic. Nanofluids at the channel entrance are considered to be hydro dynamically steady and the fully developed flow is attained at the edge of the step, and the stream wise gradients of all quantities at the channel exit where set to be zero.

This study exclusively deals with turbulent flows. The nanoparticles and the base fluid (i.e. water) are assumed to have a thermal equilibrium and no slip condition occurs. The fluid flow is assumed to be Newtonian and incompressible. Radiation heat transfer and viscous dissipation term are neglected. The internal heat generation is not conducted in this study. The thermophysical properties of the nanofluids are constant and only affected by buoyancy force, which means that the body force acting on the fluid is the gravity, the density is varied and can be adequately modeled by the Boussinesq approximation. GAMBIT and FLUENT, commercial software were used in the current study to perform the simulations [23].

$$\rho - \rho\infty = (T - T_\infty) \tag{1}$$

where ρ is density, T is temperature, β is coefficient of thermal expansion, $\rho\infty$ and $T\infty$ are ambient density and temperature, respectively. Once these assumptions are made, it is possible to derive the governing equation of the nanofluids flow over a forward double step.
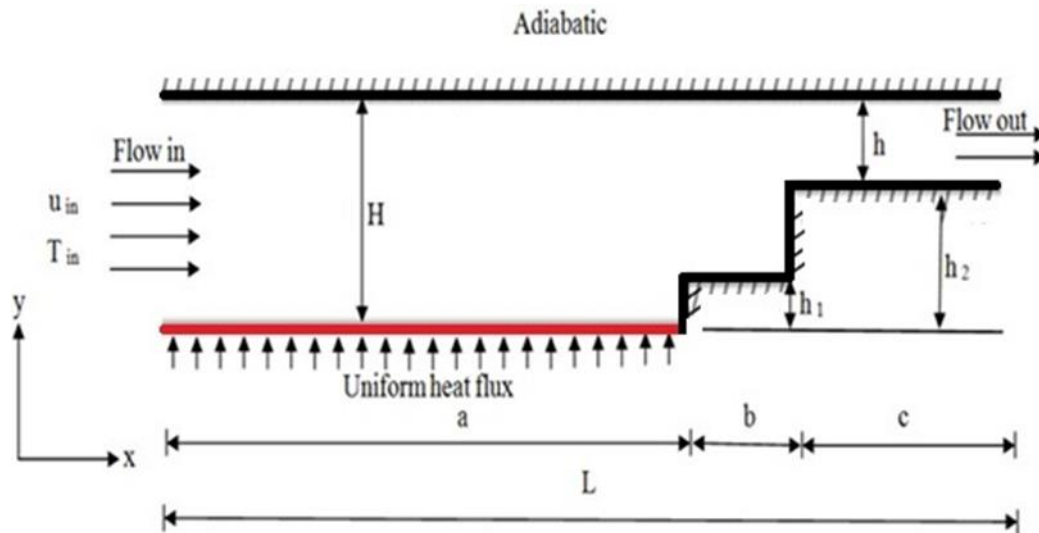
Fig. 1. Schematic diagram for 2D FFS in a channel flow

2.2 Governing Equations

To complete the CFD analysis of forward facing double steps, it is important to set up the governing equations (continuity, momentum, and energy). Using the Boussinesq approximation and neglecting the viscous dissipation effect governing equations for two dimensional laminar and turbulent incompressible flows can be written as follows [22]

The continuity equation

$$\frac{\partial u}{\partial x} + \frac{\partial v}{\partial y} = 0 \tag{2}$$

The x-momentum equation

$$U\frac{\partial u}{\partial x} + v\frac{\partial u}{\partial y} = -\frac{1}{(1-\varphi)+\varphi\frac{\rho s}{\rho f}}\frac{\partial p}{\partial x} + \frac{1}{\mathrm{Re}}\frac{1}{(1-\varphi)^{2.5}\left((1-\varphi)+\varphi\frac{\rho s}{\rho f}\right)}\left(\frac{\partial^2 u}{\partial x^2} + \frac{\partial^{2u}}{\partial y^2}\right) \tag{3}$$

The y-momentum equation

$$u\frac{\partial v}{\partial x} + v\frac{\partial v}{\partial y} = -\frac{1}{(1-\varphi)+\varphi\frac{\rho s}{\rho f}}\frac{\partial p}{\partial y} + \frac{1}{\mathrm{Re}}\frac{1}{(1-\varphi)^{2.5}\left((1-\varphi)+\varphi\frac{\rho s}{\rho f}\right)} * \left(\frac{\partial^2 v}{\partial x^2} + \frac{\partial^2 v}{\partial y^2}\right) \tag{4}$$

The energy equation

$$u\frac{\partial T}{\partial x} + v\frac{\partial T}{\partial y} = \frac{1}{\alpha}\left(\frac{\frac{k_{nf}}{k_f}}{(1-\varphi) + \varphi\frac{(\rho c_p)_S}{(\rho c_p)_f}}\right)\left(\frac{\partial^2 T}{\partial x^2} + \frac{\partial^2 T}{\partial y^2}\right) \tag{5}$$

Turbulence model equations

The turbulence model employed for turbulence flow modeling is the standard *k-ε* model. The turbulence kinetic energy, k, and the dissipation rate, *ε*, are determined using the following transport equations [23].

$$\frac{\partial}{\partial x}(\rho k u)= \frac{\partial}{\partial y}([\mu +\frac{\mu_t}{\sigma_k})\frac{\partial k}{\partial y}])+G_k - \rho\varepsilon \tag{6}$$

$$\frac{\partial}{\partial x}(\rho\varepsilon u) = \frac{\partial}{\partial y}[(\mu+\frac{\mu_t}{\sigma_\varepsilon})\frac{\partial\varepsilon}{\partial y}]+C_{1\varepsilon}\frac{\varepsilon}{k}(G_k+C_{3\varepsilon}G_b)-C_{2\varepsilon}\rho\frac{\varepsilon^2}{k} \tag{7}$$

$$\text{(a) } \mu_t= \rho C_p\frac{k^2}{\varepsilon}, \text{ (b) } G_k=-\rho v'u\frac{\partial v}{\partial x} \tag{8}$$

2.3 Boundary Conditions

Turbulent heat transfer problem considered in this paper is schematically shown in Figure 1. It is a channel with double FFS. The top wall and steps are insulated, whereas the bottom wall has heat flux which is hotter than the inlet flow temperature. Two-dimensional, steady-state, incompressible turbulent and laminar flow is considered. The channel has double FFS which their height is h_1 and h_2, respectively. Height and length of the channel are depicted by H and L, respectively. Here, b and c show the length of steps, is the length of bottom wall.

2.4 Code Validations and Grid Testing
2.4.1 Grid independence test

Grid independence tests were performed using different uniform grid densities to reach the most accurate results from the simulations. All the tests were carried out using air with Re number of 80000 at T_{in} = 20°C. Four mesh densities were examined 220 × 20, 240 × 30, 280 × 40, and 320 × 60. The uniform grid size of 280 × 40 confirms the grid independence test. Where it was found that, at the Nu corresponding to the grid density, when increase the number of intervals in both *y* and *x* direction does not affect significantly the value of Nusselt number as shown in Figure 2. This observation indicates an adequate spatial resolution of the present simulation.
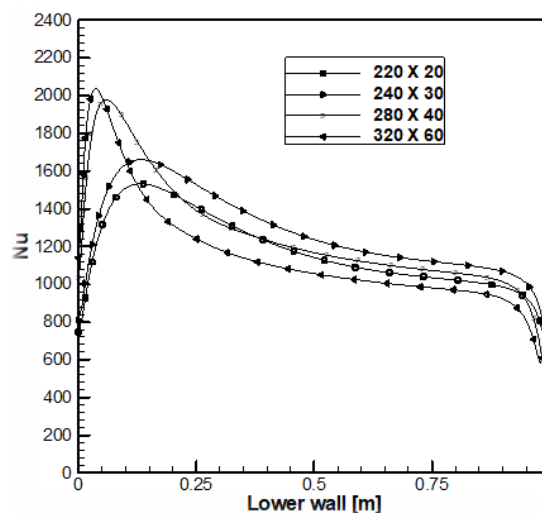

Fig. 2. Grid independence test results

2.4.2 Code validation

Code validation is very significant step in any numerical work in order to ensure that the numerical code is validated with other pervious works and it is ready for further runs. The present results obtained were compared and validated with the previous studies and acts as a benchmark for the project. On the other hand, it is not important only to get high accuracy of any numerical code but also to gain a better understanding on its capabilities and limitations.

Comparison was made in terms of Nusselt number, skin friction, and velocity distribution with results of Mohammed *et al.,* [4] as can see in Figure 3. Mohammed *et al.,* [4] used different types of nanofluids flow over backward facing step geometry which has adiabatic steps walls and heated bottom and upper walls. The comparison was carried out for Re= 225 and ΔT = 20℃ for diamonds nanofluids where laminar mixed convection flow was assumed. An excellent agreement was obtained between the present results and those of mentioned authors.
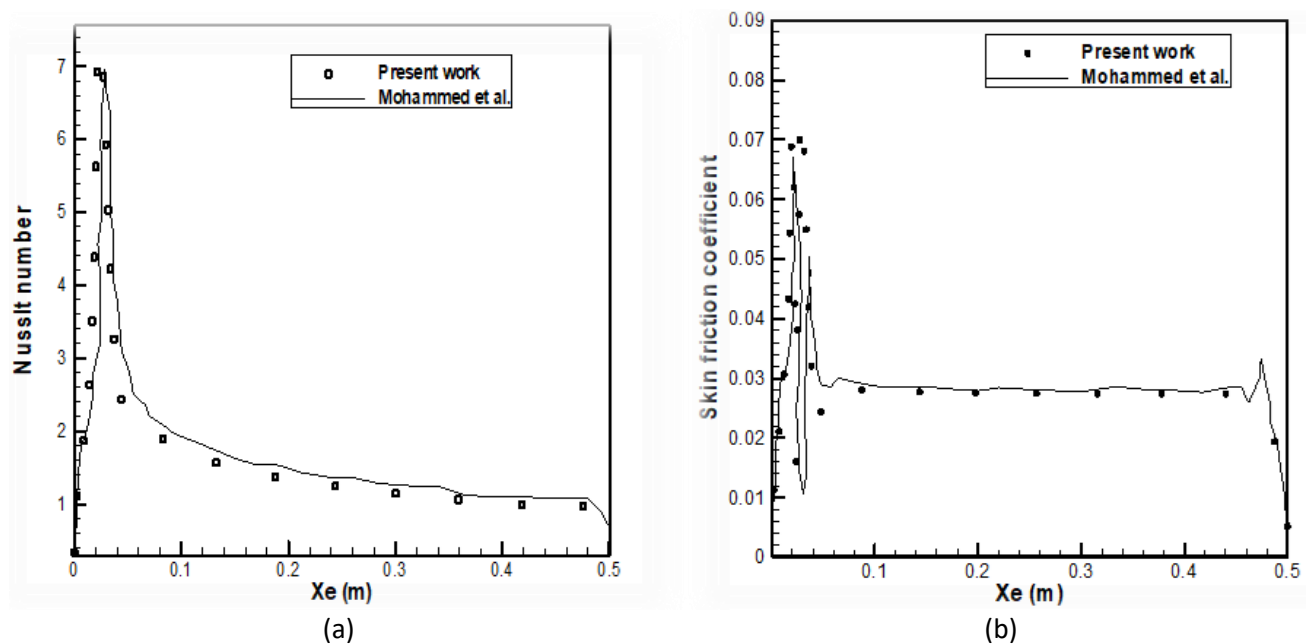

Fig. 3. Comparison of the present results with the results of Mohammed *et al.,* [4], (a) Nusselt number (b) Skin friction coefficient with Re= 225

The second validation of mixed convection flow is conducted with the results of Hong *et al.,* [19]. The Reynolds number is maintained constant at Re = 100 and uniform heat flux is fixed at q_w = 200 W/m^2 for different inclination angles (0°, 90°, 135°, 180°, 315°). The results are validated and compared as shown in Figure 4. The present results indicate a good agreement with those of Hong *et al.,* [19].

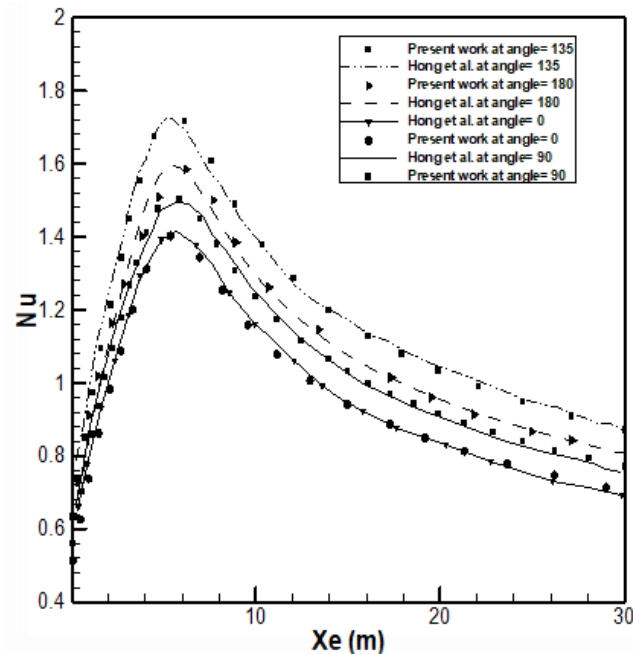**Fig. 4.** Comparison of nusselt number with the results of Hong *et al.,* [19] (S = 4.8 mm, and ER = 2) for Re = 100, and q_w = 200 W/m^2 at different inclination angles

2.5 Numerical Parameters and Procedures

The numerical computation was carried out by solving the governing conservation equations along with the boundary conditions Eq. (2)-(5). Equations for solid and fluid phase were simultaneously solved as a single domain. The discretization of governing equations in the fluid and solid regions was done using the finite-volume method (FVM). The diffusion term in the momentum and energy equations is approximated by second-order central difference which gives a stable solution. In addition, a second-order upwind differencing scheme is adopted for the convective terms. The numerical model was developed in the physical domain, and dimensionless parameters were calculated from the computed velocity and temperature distributions. The flow field was solved using the SIMPLE algorithm [24]. This is an iterative solution procedure where the computation is initialized by guessing the pressure field. Then, the momentum equation is solved to determine the velocity components. The pressure is updated using the continuity equation. Even though the continuity equation does not contain any pressure, it can be transformed easily into a pressure correction equation [25].

2.6 Thermophysical Properties of Nanofluids

In order to carry out simulations for nanofluids, the effective thermophysical properties of nanofluids must be calculated first. In this case, the nanoparticles being used,Al_2O_3, CuO, SiO_2 and ZnO. Basically the required properties for the simulations are effective thermal conductivity (k_{eff}), effective dynamic viscosity (μ_{eff}), effective mass density (ρ_{eff}), effective coefficient of thermal expansion (β_{eff}) and effective specific heat (cp_{eff}). Regarding these, the effective properties of mass density, specific heat and coefficient of thermal expansion is actually calculated according to the mixing theory.

Effective Thermal Conductivity

By using the Brownian motion of nanoparticles forward and backward double steps, the effective the thermal conductivity can be obtained using the following mean empirical correlation [26]

$$k_{eff} = k_{Static} + k_{Brownian} \tag{9}$$

Static Thermal Conductivity

$$k_{static} = k_{bf} \left[\frac{k_{np} + 2k_{bf} - 2(k_{bf} - k_{np)\emptyset}}{k_{np} + 2k_{bf} + (k_{bf} - k_{np)\emptyset}} \right] \tag{10}$$

Brownian Thermal Conductivity

$$k_{Brownian} = 5 \times 10^4 \beta \emptyset \rho_{bf} c_p, bf \sqrt{\frac{kT}{2\rho_{np}}} f(T, \emptyset) \tag{11}$$

where Boltzmann constant: $k = 1.3807 x 10^{-23} J/K$
Modeling function, β [27]

For Al_2O_3 $\beta = 8.4407(100\phi)^{-1.07304}$ 1% ≤ φ ≤ 10% 298 K ≤ T ≤ 363K

For CuO $\beta = 9.881(100\phi)^{-0.9446}$ 1% ≤ φ ≤ 6% 298 K ≤ T ≤ 363 K

For SiO_2 $\beta = 1.9526(100\phi)^{-1.4594}$ 1% ≤ φ ≤ 10% 298 K ≤ T ≤ 363K

For ZnO $\beta = 8.4407(100\phi)^{-1.07304}$ 1% ≤ φ ≤ 7% 298 K ≤ T ≤ 363 K

Modeling function, $f(T, \emptyset)$

$$f(T, \emptyset) = (2.8217 \times 10^{-2} \emptyset) + (3.917 \times 10^{-3}) \left(\frac{T}{T_0} \right) + (-3.0699 \times 10^{-2} \emptyset - 3.91123 \times 10^{-3})$$

Effective Physical Properties
By using the Brownian motion of nanoparticles in over backward and forward double steps, the effective viscosity can be obtained as following mean empirical correlation [28]

$$\text{Viscosity:} \frac{\mu_{eff}}{\mu_f} = \frac{1}{1 - 34.87 \left(\frac{d_p}{d_f} \right)^{-0.3} \emptyset^{1.03}} \tag{12}$$

where Equivalent diameter of base fluid molecule

$$d_f = \left[\frac{6M}{N\pi\rho_{bf}} \right]^{1/3} \tag{13}$$

where T is the temperature, $\emptyset$ is the particle volume fraction, M is the molecular weight of the base fluid, N is the Avogadro number, f refers to nanofluid, bf refers to base fluid and p refers to nanoparticle.

The density of the nanofluid ρ_{eff} [26]

$$\rho_{nf} = (1 - \emptyset)\rho_f + \emptyset\rho_{np} \tag{14}$$

whereby ρ_f and ρ_{np} are the mass densities of the base fluid and the solid nanoparticles, respectively.

The effective Heat capacity at constant pressure of the nanofluid, $(\rho c p)_{nf}$ [26]

$$(\rho c_p)nf = (1 - \emptyset)(\rho c_p)f + \emptyset(\rho c_p)np \tag{15}$$

when $(\rho_{c_p})_f$ and $(\rho c_p)_{np}$ are heat capacities of base fluid and nanoparticles, respectively.
The effect coefficient of thermal expansion of nanofluid, $(\rho\beta)_{nf}$ [26]:

$$(\rho\beta)_{nf} = (1 - \emptyset)(\rho\beta)_f + \emptyset(\rho\beta)_{np} \tag{16}$$

when $(\rho\beta)_f$ and $(\rho\beta)_{np}$ are thermal expansion coefficients of base fluid and nanoparticles, respectively.

Table 1 shows thermophysical properties for pure water, different nanofluids and different base fluids at T = 300K [26]

Table 1
Thermophysical properties for pure water, different nanofluids and different base fluids at T = 300K [26]

Properties	Water	Al$_2$O$_3$	CuO	ZnO	SiO$_2$	Glycerin	Engine oil	Ethylene glycol
$\rho(kg/m^3)$	988.203	3970	6500	5600	2200	1259.9	884.1	1114.4
$\mu,(Ns/m^2)$	0.001	-	-	-	-	79.9	0.486	0.0152
$k(W/m.K)$	0.613	40	20	13	1.2	0.286	0.145	0.252
cp$(J/kg.K)$	4182.2	765	535.6	495.2	703	2427	1909	2415
$\beta(1/K)$	0.000206	0.000005	0.000004	0.000004	0.000005	0.00048	0.0007	0.00065

3. Result and Discussion
3.1 The Effect of Different Types of Nanofluids
3.1.1 Nusselt number

In this section, four different types of nanoparticles which are Al_2O_3 , CuO, SiO_2 and ZnO and pure water as a base fluid on local Nusselt number over the bottom wall was presented. The Nusselt number for different nanofluids at Re = 80000, while volume fraction and particle diameter are 4% and 20 nm are shown in Figure 5. As can see similar trends of Nusselt number are obtained for all nanofluid. But in case of comparing among the four types of nanofluids, it is clear that the nanofluid with SiO_2 has the highest Nu number, followed by Al_2O_3, CuO and ZnO respectively. Nanofluids with higher Prandtl number have higher Nusselt number along the heated. Base fluid with SiO_2 nanoparticle has the highest Nusselt number values amaong the rest nanofluids, due to its highest thermal properties compared to the other nanofluids investigated, followed by Al_2O_3 then ZnO and finally CuO with least value.
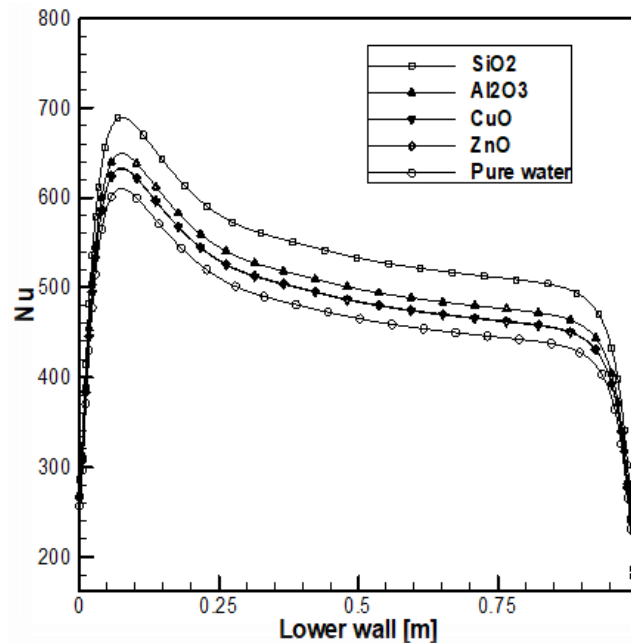
Fig. 5. Local Nusselt number for different nanofluids along the heated bottom wall Re = 80000 and with d_p = 20 nm and $\emptyset$ = 4%

3.1.2 Skin friction coefficient

The skin friction coefficient of base fluid with different nanoparticles at Re = 80000 and T_∞ = 300K at the inlet, heat flux is q_w = 200 W/m^2 along the heated wall with nanoparticle size of 20 nm and volume fraction of 4% is shown in Figure 6. It is noticed that the skin friction is similar in the trend of local Nusselt number at that wall. Then, it slightly increases at the vicinity of duct's inlet section. After that, the skin friction coefficient decreases along the flow direction until it becomes minimum at the reattachment point where the velocity almost zero. This decrement caused by decreasing the dynamic pressure. It is shown that downstream the reattachment point, the skin friction coefficient increases until it reaches to another maximum. This peak occurs due to the recirculation flow where there is change in the velocity. After that the skin friction coefficient diminishes steeply until it reaches to the first step edge. The effect of skin friction coefficient for different nanofluids is insignificant and the difference is not clear because their results are much closed to each other.
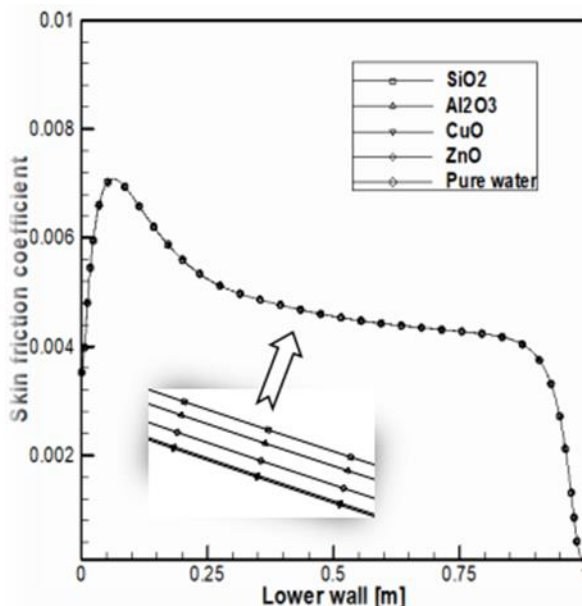
Fig. 6. Skin friction coefficient for different nanofluids along the heated bottom wall at Re = 80000 with d_p = 20 nm and $\emptyset$ = 4%

3.1.3 Velocity distribution

The velocity distributions of different nanofluids with φ = 4% for *Re* = 80000, d_p = 20 nm for different X/H sections along the down-stream wall is shown in Figure 7(a)-(b). It is clear from the figures at X/H = 1 and X/H = 30 that nanofluids with low density such as SiO_2 have higher velocity distribution at the edge of the baffle wall than those with high density such as CuO at constant Reynolds number. The flow is observed behind the step wall due to the recirculation region that attached to the step and the vortex which leaves the recirculation region and changes its direction down-stream the channel duo to the buoyancy force. Figure 8 shows streamlines and isotherms for SiO_2 nanofluids flow with $\emptyset$ = 4% for Re = 80000, dp = 20 nm.
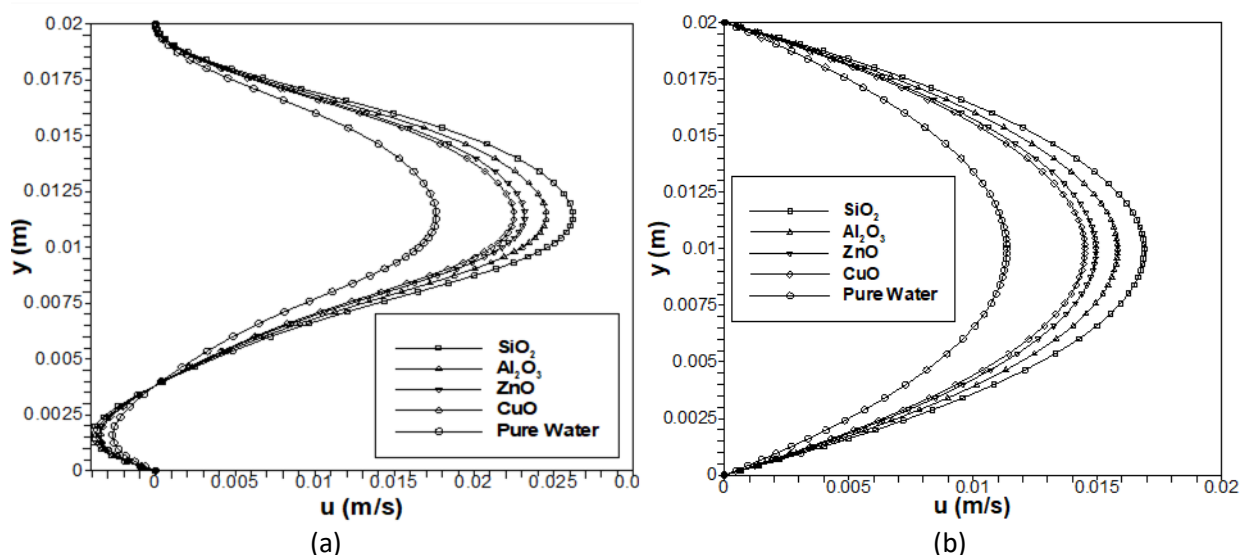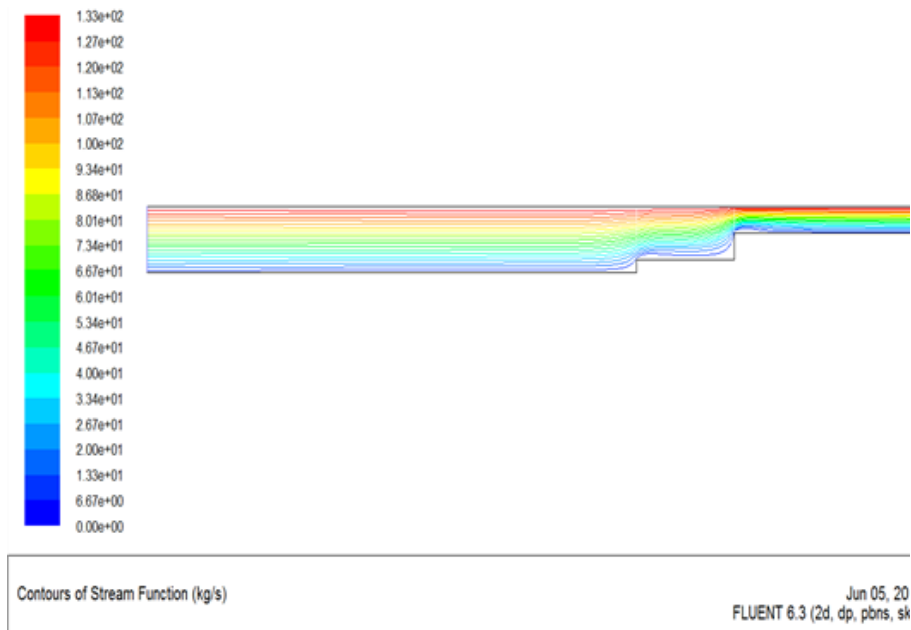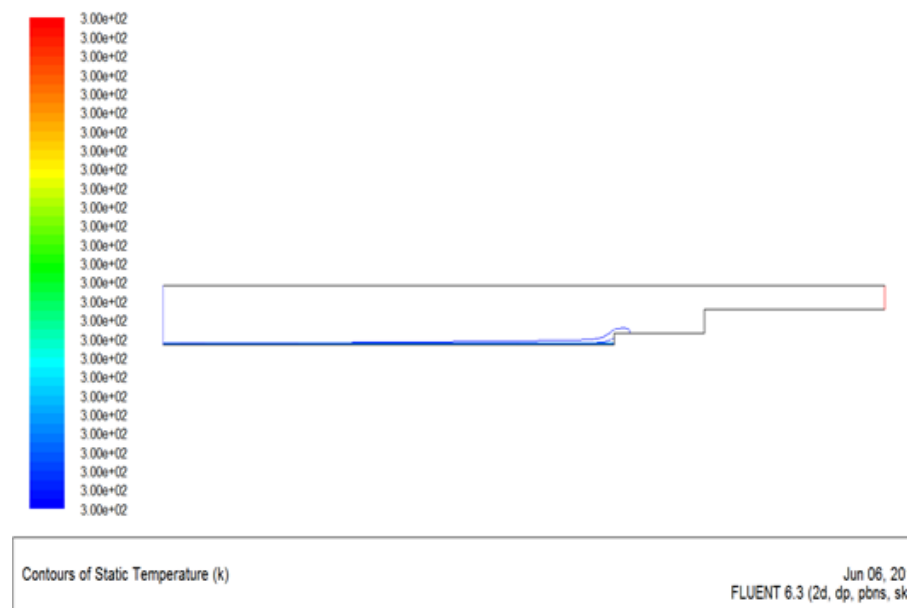

(a)

(b)

Fig. 7. Velocity distributions of different nanofluids with $\emptyset$ = 4% for Re = 1000, d_p = 20 nm and at (a) X/H = 9, (b) X/H = Exit

Contours of Stream Function (kg/s)

Jun 05, 20
FLUENT 6.3 (2d, dp, pbns, sk

(a)

Contours of Static Temperature (k)

Jun 06, 20
FLUENT 6.3 (2d, dp, pbns, sk

(b)

Fig. 8. (a) Streamlines and (b) isotherms for SiO_2 nanofluids flow with $\emptyset$ = 4% for Re = 80000, d_p = 20 nm

3.2 The Effect of Different Volume Fractions of Nanoparticles

The volume fraction of nanoparticles is actually referred to the volume of nanoparticles constituent divided by the volume of all constituents of the mixture prior to mixing. Volume fraction of nanofluids is the ratio of nanoparticles suspended in base fluids. Thus, pure water has zero volume fractions. In this study the volume fraction was in the range of $0 - 4\%$ with Re = 80000 and nanoparticle diameter d_p = 20 nm of (SiO_2) nanofluid is studied and Nusselt number for this condition is shown in Figure 9. Hence, nanofluids with higher volume fraction bring grater heat transfer enhancement. Because increasing the volume fraction leads to increase the thermal conductivity of the fluid.
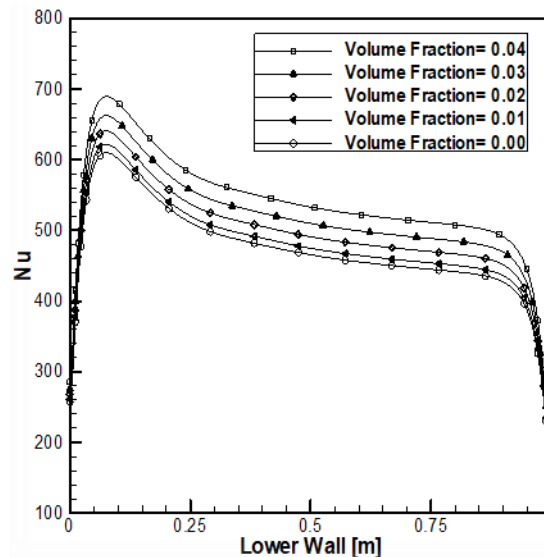
Fig. 9. Local Nusselt number for different volume fractions along the heated bottom wall of SiO_2 nnanofluids flow with Re = 80000 at d_p = 20 nm

3.3 The Effect of Different Nanoparticles Diameters

This study is used SiO_2- water as working fluid with volume fraction ($\emptyset$ = 4%) at Re = 80000. The range of nanoparticles diameter is used 20 – 80 nm. As illustrated in Figure 10. The results show that the Nusselt number increases with decreasing the nanoparticles diameter. This can be attributed to the increment of the thermal conductivity due to nanoparticles diameter decrease. The unique features of nanofluid come from relatively high surface area to volume ratio of nanoparticles.
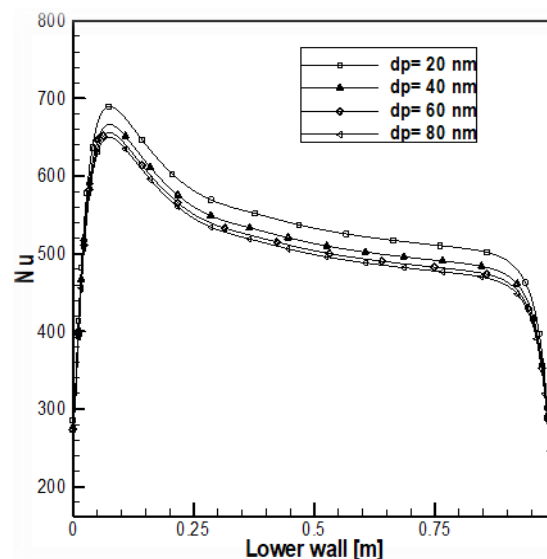

Fig. 10. Local Nusselt number for different nanoparticle diameters along the heated bottom wall of SiO_2 nanofluids flow with Re = 80000 at $\emptyset$ = 4%

Basically, as heat transfer focused on the surface of the nanoparticles, it desirable to use particles that possess high surface area to volume ratio, it is lead to higher heat transfer coefficient. Hence, it is concluded that by using smaller diameter of nanoparticles will lead to get better heat transfer enhancement.

3.4 The Effect of Different Reynolds Numbers, Re
3.4.1 Nusselt number

This study was done at Reynolds number in the range of 4000 – 100000 turbulent flow with volume fraction ($\emptyset = 4\%$) and nanoparticles size d_p= 20 nm at horizontal position of SiO_2 nanofluid along the bottom heated wall is presented in Figure 11. At different values of Re, similar trends are obtained for the variation of Nu. As expected, increasing Re leads to increase the value of Nu along the heated lower wall.
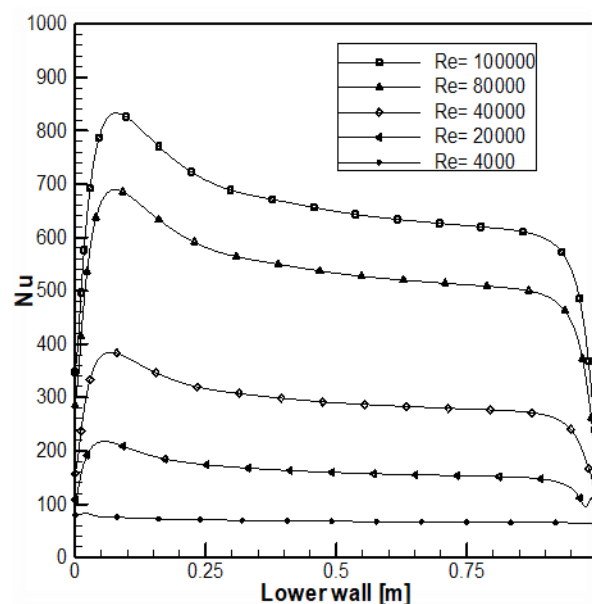

Fig. 11. Local Nusselt number along the heated bottom wall for different Reynolds numbers of SiO_2 nanofluid with turbulent flow at $\emptyset$ = 4% and d_p = 20 nm

3.4.2 Skin friction coefficient

The skin friction of SiO_2 nanofluid with volume fraction ($\emptyset$ = 4%), nanoparticle size (d_p = 20 nm) for different Reynolds numbers in the range of 4000 – 100000 turbulent flow at heat flux ($q_w = 200$ W/m^2) along bottom wall is shown in Figure 12. It is observed that the skin friction decreases as Reynolds number increases. The trend of the skin friction coefficient is discussed in detail, previously. Therefore, as the velocity increases; the magnitude of Reynolds number increases and skin friction coefficient decreases. Because the skin friction coefficient is inversely proportional to the velocity.
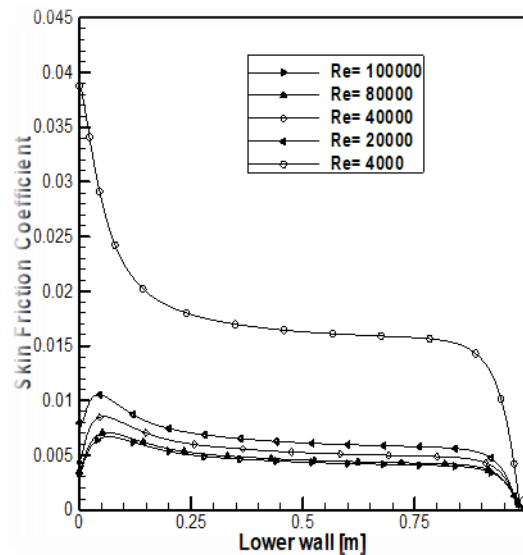
Fig. 12. Skin friction coefficient along the heated bottom wall for different Reynolds numbers of SiO_2 nanofluid with turbulent flow at $\emptyset$ = 4% and d_p = 20 nm

3.4.3 Velocity distribution

The velocity distribution for different Reynolds numbers ranged between 4000 to 100000 of SiO_2 nanofluid with $\emptyset$ = 4%, $q_w = 200$ W/m^2 at bottom wall and d_p = 20 nm at different X/H is shown Figure 13. The velocity profile increases as Reynolds number increases. In addition, the size of all recirculation zones increases by increasing Re due to the increment in the velocity. Streamlines and isotherms are shown in Figure 14 which shows the development of these vortices.
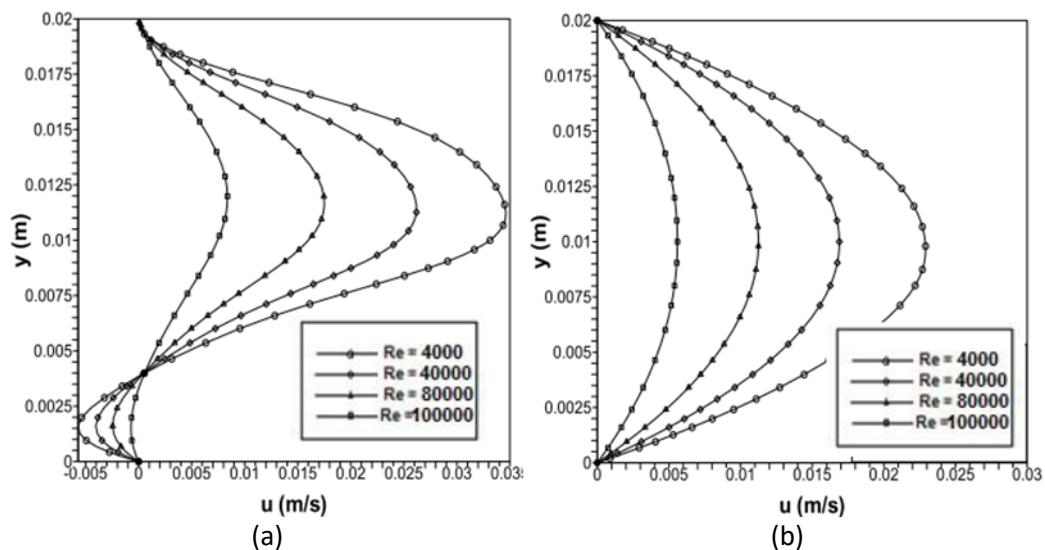

(a)   (b)

Fig. 13. Velocity distribution of SiO_2 nanofluid for different Reynolds number with $\emptyset$ = 4% and d_p = 20 nm at (a) X/H = 9, (b) X/H = Exit
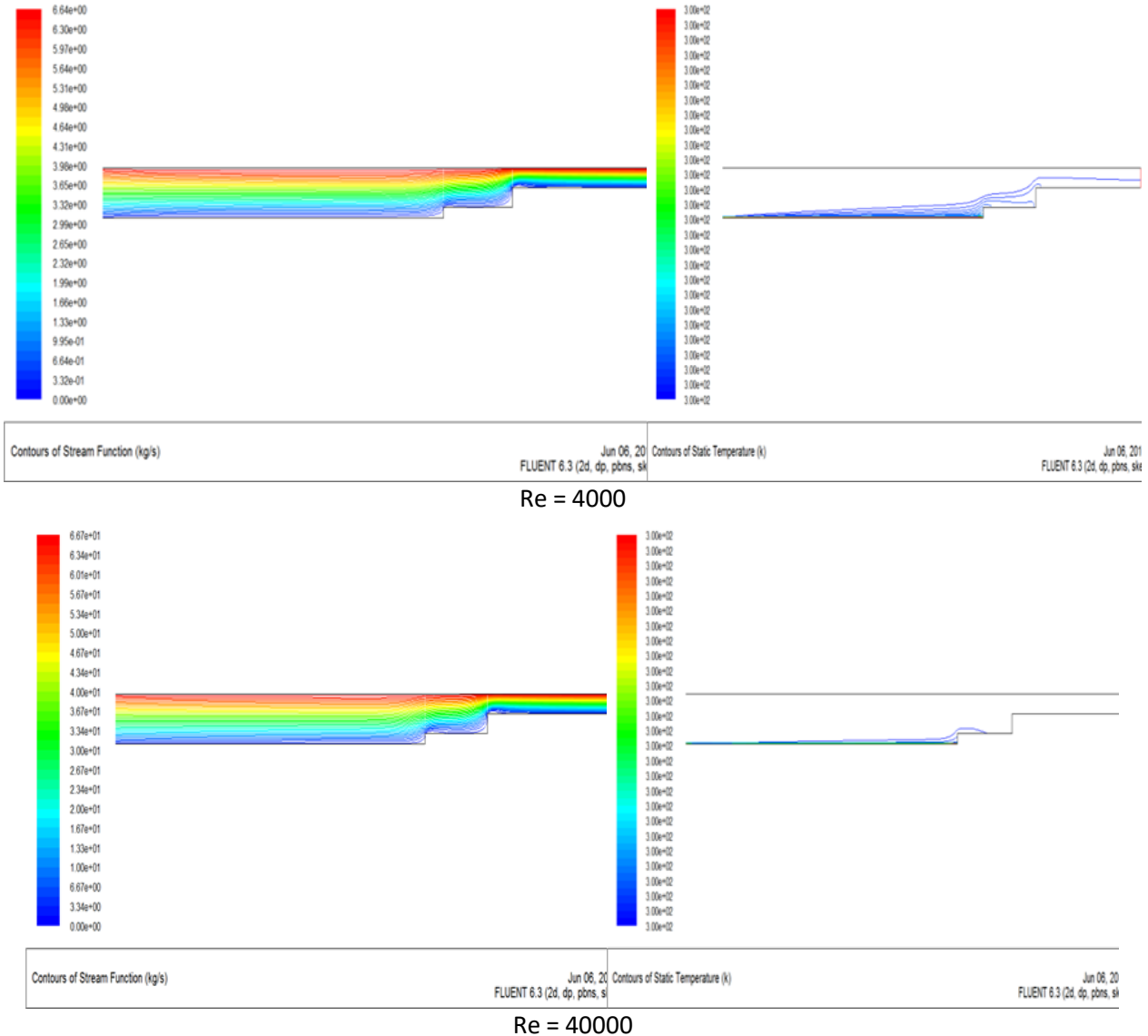
Fig. 14. Streamlines(left) and isotherms (right) for different Reynolds numbers of SiO_2 nnanofluids flow with $\emptyset$ = 4%, d_p = 20 nm

3.5 The Effect of Step Height

The effect of the two steps heights on Nusselt number distribution of SiO_2 nanofluid with $\emptyset$ = 4%, $q_w = 200$ W/m^2 in bottom wall and d_p = 20 at Re = 80000 and step heights in the range of 0.01m $\leq$ $h_1 \leq 0.04$m and 0.03m $\leq h_2 \leq 0.06$m is presented in Figure 15. It is shown that there is no considerable influence of the steps height on the Nusselt number. It is noted that the fact for high convective flow, importance effects move only from upstream, hence makes the space coordinate almost one way.
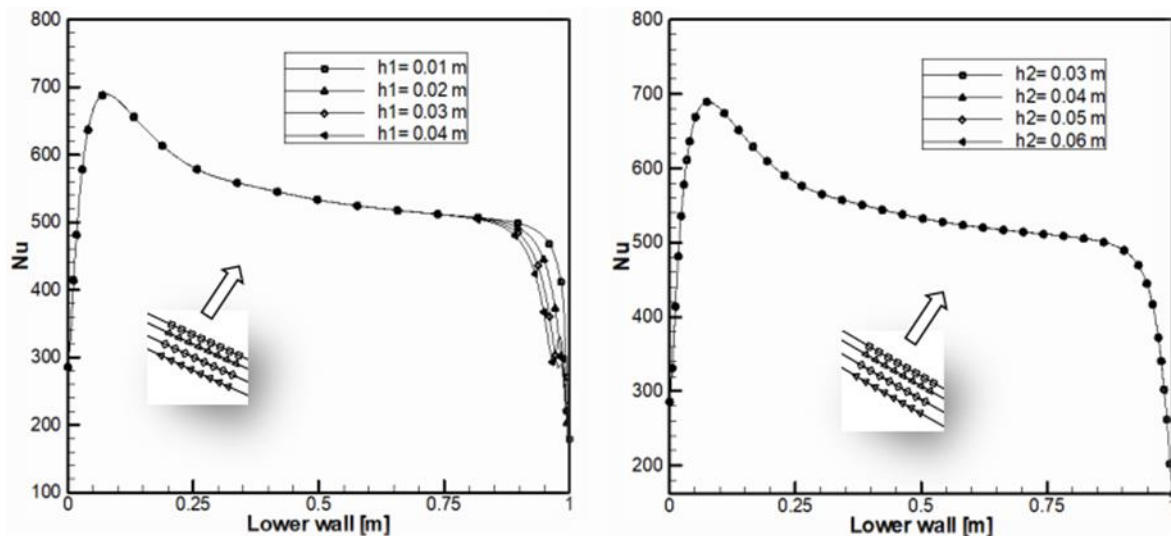
Fig. 15. Nusselt number for different steps heights of two steps (left) first step h_1, and (right) second step h_2 of SiO_2 nanofluid at Re = 80000

3.7 The Effect of Different Base Fluids

In this study, four different types of base fluids which are fluids (pure water, ethylene glycol, engine oil and glycerin) are used. In order to see the effects of different base fluids on heat transfer enhancement all other parameters should be fixed. The Nusselt Number for different base fluids at Re = 80000, $\emptyset$ = 4%, d_p = 20 nm and T_∞ = 300K are shown in Figure 16. This figure shows for all four base fluids possess higher Nusselt number compare between them. But in comparing among the four types of base fluids, it is clear that the glycerin has highest Nusselt number followed by engine oil, ethylene glycol and pure water respectively. This phenomenon can be attributed to fact of the high thermal properties of the glycerin compare with lower thermal properties of other base fluids types.
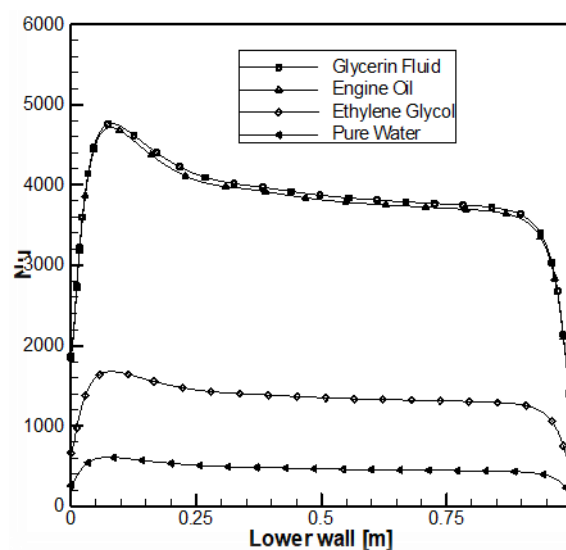

Fig. 16. Nusselt number along the heated bottom wall for different base fluids with Re = 80000, d_p = 20 nm, $\emptyset$ = 4%, at T_∞ = 300K

4.Conclusions

Numerical simulation of mixed convection heat transfer in inclined forward double steps using nanofluids was presented. The emphasis is given on the heat transfer enhancement resulting from various parameters, which include different nanofluids (Al_2O_3, CuO, SiO_2 and ZnO with base fluid (water, ethylene glycol, engine oil and glycerin), nanoparticles diameter in range of $20 \leq dp \leq 80$ nm, volume fraction (concentration) in the range of $0 \leq \emptyset \leq 4\%$, Reynolds number for turbulent flow, Re in the range of $4000 \leq Re \leq 100000$, steps heights for forward double steps in the range of 0.01 m $\leq h_1 \leq 0.04$ m, and 0.03 m $\leq h_2 \leq 0.06$ m. The governing equations were solved using finite volume method with certain assumptions and appropriate boundary conditions to provide a clear understanding of the modeling aims and conditions for the present study.

It is found that the changing the types of nanoparticles, Al_2O_3, CuO, SiO_2 and ZnO, the results show that SiO_2 gives the highest Nusselt number followed by Al_2O_3, CuO and ZnO, respectively while pure water gives the lowest Nusselt number and the Nusselt number is found to increase with increasing the volume fraction of nanoparticles**.** The Nusselt number increased gradually when decreasing the nanoparticles diameter**.** It is found that there is no considerable influence of the steps height on the Nusselt number. The skin friction coefficient decreased with increasing Reynolds number and it has about same variation along the heated wall for different nanofluids, and The Nusselt number increased gradually by increasing the Reynolds number. The investigations of this work will surely solve many heat transfer related problems in the near future and are very likely to apply in the numerous practical heat transfer devices.

References

[1]   Griebel, Michael, Thomas Dornseifer, and Tilman Neunhoeffer. *Numerical simulation in fluid dynamics: a practical introduction*. Vol. 3. Siam, 1997.

[2]   Solangi, K. H., S. N. Kazi, M. R. Luhur, A. Badarudin, A. Amiri, Rad Sadri, M. N. M. Zubir, Samira Gharehkhani, and K. H. Teng. "A comprehensive review of thermo-physical properties and convective heat transfer to nanofluids." *Energy* 89 (2015): 1065-1086.

[3]   Wang, Xiang-Qi, and Arun S. Mujumdar. "Heat transfer characteristics of nanofluids: a review." *International journal of thermal sciences* 46, no. 1 (2007): 1-19.

[4]   Mohammed, H. A., A. A. Al-Aswadi, H. I. Abu-Mulaweh, Ahmed Kadhim Hussein, and P. Rajesh Kanna. "Mixed convection over a backward-facing step in a vertical duct using nanofluids—buoyancy opposing case." *Journal of Computational and Theoretical Nanoscience* 11, no. 3 (2014): 860-872.

[5]   Fathinia, F., and Ahmed Kadhim Hussein. "Effect of Blockage Shape on Unsteady Mixed Convective Nanofluid Flow Over Backward Facing Step." *CFD Letters* 10, no. 1 (2018): 1-18.

[6]   Abu-Mulaweh, H. I. "Turbulent mixed convection flow over a forward-facing step—the effect of step heights." *International Journal of Thermal Sciences* 44, no. 2 (2005): 155-162.

[7]   Abu-Mulaweh, H. I. "Effects of backward-and forward-facing steps on turbulent natural convection flow along a vertical flat plate." *International journal of thermal sciences* 41, no. 4 (2002): 376-385.

[8]   Hussain, Omar A. and Thamer Khalif Salem. "Mixed Convective Nanofluids over Vertical Channel Having Forward-Facing Step Flow Having a Baffle." *Journal of Advances in Technology and Engineering Research* 2, no. 6 (2017).

[9]   Chiba, Kunji, Ryuta Ishida, and Kiyoji Nakamura. "Mechanism for entry flow instability through a forward-facing step channel." *Journal of non-newtonian fluid mechanics* 57, no. 2-3 (1995): 271-282.

[10] Saqr, Khalid M., Hossam S. Aly, Malzan A. Wahid, and Mohsin M. Sies. "Numerical simulation of confined vortex flow using a modified k-epsilon turbulence model." *CFD letters* 1, no. 2 (2010): 87-94.

[11] Hattori, Hirofumi, and Yasutaka Nagano. "Investigation of turbulent boundary layer over forward-facing step via direct numerical simulation." *International Journal of Heat and Fluid Flow* 31, no. 3 (2010): 284-294.

[12]   Largeau, J. F., and V. Moriniere. "Wall pressure fluctuations and topology in separated flows over a forward-facing step." *Experiments in Fluids* 42, no. 1 (2007): 21-40.

[13] Öztop, Hakan F. "Turbulence forced convection heat transfer over double forward facing step flow." *International communications in heat and mass transfer* 33, no. 4 (2006): 508-517.

[14] Dutta, Prashanta, and Sandip Dutta. "Effect of baffle size, perforation, and orientation on internal heat transfer

enhancement." *International Journal of Heat and Mass Transfer* 41, no. 19 (1998): 3005-3013.

[15] Yang, Yue-Tzu, and Chih-Zong Hwang. "Calculation of turbulent flow and heat transfer in a porous-baffled channel." *International Journal of Heat and Mass Transfer* 46, no. 5 (2003): 771-780.

[16] Hussein, Omar A. "Laminar Mixed Convective Nanofluid Flow in a Channel with Double Forward-Facing Steps: A Numerical Simulation Study." *Tikrit Journal of Engineering Sciences* 24, no. 1 (2017): 38-49.

[17] Nie, Jian H., Y. T. Chen, and Hsuan-Tsung Hsieh. "Effects of a baffle on separated convection flow adjacent to backward-facing step." *International Journal of Thermal Sciences* 48, no. 3 (2009): 618-625.

[18] Kherbeet, A. Sh, H. A. Mohammed, and B. H. Salman. "The effect of nanofluids flow on mixed convection heat transfer over microscale backward-facing step." *International Journal of Heat and Mass Transfer* 55, no. 21-22 (2012): 5870-5881.

[19] Hong, B., Bassem F. Armaly, and T. S. Chen. "Laminar mixed convection in a duct with a backward-facing step: the effects of inclination angle and Prandtl number." *International journal of heat and mass transfer* 36, no. 12 (1993): 3059-3067.

[20] Mohammed, H. A., and Omar A. Hussein. "Assisting and Opposing Combined Convective Heat Transfer and Nanofluids Flows Over a Vertical Forward Facing Step." *Journal of Nanotechnology in Engineering and Medicine* 5, no. 1 (2014): 010903.

[21] Chiang, T. P., Tony WH Sheu, and S. F. Tsai. "Topological flow structures in backward-facing step channels." *Computers & fluids* 26, no. 4 (1997): 321-337.

[22] Abu-Nada, Eiyad. "Application of nanofluids for heat transfer enhancement of separated flows encountered in a backward facing step." *International Journal of Heat and Fluid Flow* 29, no. 1 (2008): 242-249.

[23] Anderson, John David, and J. Wendt. *Computational fluid dynamics*. Vol. 206. New York: McGraw-Hill, 1995.

[24] Yılmaz, I·lker, and Hakan F. "Turbulence forced convection heat transfer over double forward facing step flow." *International communications in heat and mass transfer* 33, no. 4 (2006): 508-517.

[25] Hsu, Chia-Jung. "Numerical heat transfer and fluid flow." *Nuclear Science and Engineering* 78, no. 2 (1981): 196-197.

[26] Ghasemi, B., and S. M. Aminossadati. "Brownian motion of nanoparticles in a triangular enclosure with natural convection." *International Journal of Thermal Sciences* 49, no. 6 (2010): 931-940.

[27] Vajjha, Ravikanth S., and Debendra K. Das. "Experimental determination of thermal conductivity of three nanofluids and development of new correlations." *International Journal of Heat and Mass Transfer* 52, no. 21-22 (2009): 4675-4682.

[28] Corcione, Massimo. "Heat transfer features of buoyancy-driven nanofluids inside rectangular enclosures differentially heated at the sidewalls." *International Journal of Thermal Sciences* 49, no. 9 (2010): 1536-1546.